Acta Biomaterialia 10 (2014) 4961–4970

Contents lists available at ScienceDirect

Acta Biomaterialia

journal homepage: www.elsevier.com/locate/actabiomat

Mineralized gelatin methacrylate-based matrices induce osteogenic differentiation of human induced pluripotent stem cells

Heemin Kang [a,b], Yu-Ru V. Shih [a], Yongsung Hwang [a], Cai Wen [a,c], Vikram Rao [a], Timothy Seo [a,d], Shyni Varghese [a,b,d,*]

[a] Department of Bioengineering, University of California, San Diego, La Jolla, CA 92093, USA
[b] Materials Science and Engineering Program, University of California, San Diego, La Jolla, CA 92093, USA
[c] School of Chemistry and Chemical Engineering, Southeast University, Nanjing 210018, China
[d] Department of Nanoengineering, University of California, San Diego, La Jolla, CA 92093, USA

ARTICLE INFO

Article history:
Received 16 April 2014
Received in revised form 16 July 2014
Accepted 10 August 2014
Available online 18 August 2014

Keywords:
Human induced pluripotent stem cells
Osteogenic differentiation
Calcium phosphate
Bone tissue engineering
Gelatin methacrylate

ABSTRACT

Human induced pluripotent stem cells (hiPSC) are a promising cell source with pluripotency and self-renewal properties. Design of simple and robust biomaterials with an innate ability to induce lineage-specificity of hiPSC is desirable to realize their application in regenerative medicine. In this study, the potential of biomaterials containing calcium phosphate minerals to induce osteogenic differentiation of hiPSC was investigated. hiPSC cultured using mineralized gelatin methacrylate-based matrices underwent osteogenic differentiation *ex vivo*, in both two-dimensional and three-dimensional cultures, in growth medium devoid of any osteogenic-inducing chemical components or growth factors. The findings that osteogenic differentiation of hiPSC can be achieved through biomaterial-based cues alone present new avenues for personalized regenerative medicine. Such biomaterials that could not only act as structural scaffolds, but could also provide tissue-specific functions such as directing stem cell differentiation commitment, have great potential in bone tissue engineering.

1. Introduction

Human pluripotent stem cells (hPSC), which include both embryonic stem cells and induced pluripotent stem cells, play an important role in regenerative medicine, developmental biology and pathology, and drug screening, owing to their ability to give rise to any cells in the human body and indefinitely self-renew [1,2]. hiPSC developed from human autologous somatic cells could circumvent concerns regarding immune properties and ethical issues, making them an ideal cell source for regenerative medicine [3]. Despite the benefits that hiPSC offer, controlling their differentiation into targeted cell type(s) remains a challenge. Studies over the years have shown that stem cells respond to their microenvironment, composed of soluble and matrix-based cues, to regulate their fate and commitment [4–6]. Synthetic biomaterials have been used extensively to recapitulate tissue-specific physicochemical cues to direct self-renewal and differentiation of stem cells [7,8].

Biomaterials containing calcium phosphate minerals have been shown to promote osteogenic differentiation of stem cells [9–14]. These materials have also been shown to support *in vivo* bone tissue formation [11–15]. Previously, it has been shown that hydrogels containing acryloyl-6-aminocaproic acid (A6ACA) moieties promote their mineralization when exposed to a medium containing Ca^{2+} and PO_4^{3-} [16]. The carboxyl groups of A6ACA moieties bind to Ca^{2+} ions and promote nucleation and growth of calcium phosphate (CaP) minerals. Employing biomineralized poly(ethylene glycol)-diacrylate-*co*-acryloyl-6-aminocaproic acid (PEGDA-*co*-A6ACA) matrices, it has been shown that mineralized matrices can direct osteogenic differentiation of human bone marrow-derived mesenchymal stem cells (hMSC) and human embryonic stem cells (hESC) [10,17]. However, it required the biomineralized PEGDA-*co*-A6ACA matrices to be coated with Matrigel to promote initial attachment of the hESC to the matrix. In this study, mineralized matrices containing gelatin methacrylate (GelMA) were developed, and their potential to direct osteogenic differentiation of hiPSC was examined. Gelatin, derived from natural collagen, possesses cell adhesion motifs that could promote adhesion of hiPSC to the underlying matrix [18,19]. Moreover, gelatin-based matrices have been demonstrated to degrade [19–24] and have been studied extensively as a scaffold for tissue engineering [20,21,23,25].

Studies that have reported osteogenic differentiation of hiPSC often used derivation of MSC or mesoderm-like progenitor cells

* Corresponding author at: Department of Bioengineering, University of California, San Diego, 9500 Gilman Drive, Mail Code 0412, La Jolla, CA 92093, USA. Tel.: +1 858 822 7920; fax: +1 858 534 5722.
E-mail address: svarghese@ucsd.edu (S. Varghese).

http://dx.doi.org/10.1016/j.actbio.2014.08.010
1742-7061/

and their subsequent differentiation into osteoblasts, using osteogenic-inducing soluble factors such as β-glycerophosphate, ascorbic acid 2-phosphate, dexamethasone and/or growth factors such as bone morphogenetic protein-2 (BMP-2) [26–32]. A recent study by de Peppo et al. [27] employed decellularized bone matrix to create bone tissues from hiPSC-derived mesoderm progenitor cells. However, to the present authors' knowledge, there are no reports showing osteogenic differentiation of hiPSC solely through biomaterial-based cues. The present study demonstrates that biomaterials containing CaP minerals induce osteogenic differentiation of hiPSC in growth medium devoid of any osteogenic-inducing small molecules or growth factors.

2. Materials and methods

2.1. Synthesis and modification of materials

PEGDA (M_n = 3.4 kDa) and *N*-acryloyl 6-aminocaproic acid (A6ACA) were synthesized as previously described [17,33,34]. GelMA was prepared through methacrylation of gelatin (Sigma-Aldrich, catalog number: G1890) [19]. Briefly, 10 g of gelatin along with 100 ml of phosphate buffered saline (PBS) was added to a round-bottom flask purged with argon gas and dissolved under stirring at 60 °C. Around 8 ml of methacrylic anhydride (Polysciences, catalog number: 01517) was added dropwise under stirring for 2 h. The reaction mixture was kept at 60 °C for another 1 h, then 100 ml of PBS pre-warmed at 60 °C was added to the mixture and maintained at 60 °C for 15 min. The resulting GelMA was placed in a dialysis tube (Spectrum Laboratories, catalog number: 132676) in deionized (DI) water at 40 °C for 7 days with two daily changes of DI water and filtered through 40-μm-sized pores, lyophilized and stored at −20 °C prior to use.

2.2. Synthesis of GelMA-co-A6ACA hydrogels

GelMA-*co*-A6ACA hydrogels were synthesized as follows: 30 w/v% GelMA was dissolved in DI water at 45 °C and 1 M A6ACA was dissolved in 1 M NaOH to deprotonate the carboxyl groups. One part each of 30 w/v% GelMA and 1 M A6ACA were mixed to yield a solution containing 15 w/v% GelMA and 0.5 M (equivalent to 9 w/v%) A6ACA. Around 0.3 w/v% of photoinitiator, 1-[4-(2-hydroxyethoxy)-phenyl]-2-hydroxy-2-methyl-1-propane-1 (Ciba Specialty Chemicals, Irgacure 2959), in 70% ethanol was added to the above solution. The solution was then dispensed into a Bio-Rad glass plate separated by a 1-mm spacer and allowed to polymerize at 25 °C under 365 nm UV light for 10 min. The resultant hydrogels were incubated in PBS for 24 h with two changes of PBS. Hydrogels disks 1 cm^2 (area) × 1 mm (height) were used for the cell culture experiments.

2.3. Synthesis of GelMA-co-A6ACA-co-PEGDA macroporous hydrogels

GelMA-*co*-A6ACA-*co*-PEGDA macroporous hydrogels were synthesized using the polymethylmethacrylate (PMMA) leaching method [35]. First, 8-mm-diameter cylindrical molds packed with PMMA were made from PMMA microspheres with 165 μm in diameter (Bangs Laboratories, catalog number: BB05 N). Each PMMA column was exposed to 60 μl of 20% acetone/80% ethanol mixture for 1 min to fuse the PMMA beads. The mold was dried at 80 °C for 1 h and stored at room temperature. Next, 50 μl of a precursor solution containing 10 w/v% GelMA, 9 w/v% A6ACA (treated with NaOH), 10 w/v% PEGDA, and 0.3 w/v% Irgacure 2959 (in 70% ethanol) was dispensed into PMMA-filled molds and photopolymerized for 10 min using UV light. The PMMA beads embedded within the GelMA-*co*-A6ACA-*co*-PEGDA networks were subsequently dissolved in acetone for 3 days, while replenishing fresh acetone three times each day, yielding the macroporous hydrogels. The resultant macroporous hydrogels were gradually hydrated from pure acetone to acetone/DI water mixture and to pure DI water for a day. The macroporous hydrogels were equilibrated in PBS for 6 h and punched out to obtain constructs with diameter and height dimensions of 5 mm and 2 mm, respectively.

2.4. Mineralization and sterilization of GelMA-co-A6ACA hydrogels and GelMA-co-A6ACA-co-PEGDA macroporous hydrogels

GelMA-*co*-A6ACA hydrogels and GelMA-*co*-A6ACA-*co*-PEGDA macroporous hydrogels were subjected to the mineralization process, as described elsewhere [17]. Briefly, both matrices were soaked in DI water for 6 h and immersed in modified simulated body fluid (m-SBF; pH = 7.4) at 25 °C for 6 h. The m-SBF solution is composed of 142.0 mM Na^+, 5.0 mM K^+, 1.5 mM Mg^{2+}, 2.5 mM Ca^{2+}, 103.0 mM Cl^-, 10.0 mM HCO_3^-, 1.0 mM HPO_4^{2-} and 0.5 mM SO_4^{2-}, as described elsewhere [36]. The matrices were briefly rinsed with DI water and soaked in 40 mM Ca^{2+} and 24 mM HPO_4^{2-} solution (pH = 5.2) at 25 °C for 45 min using a VWR Mini Shaker (catalog number: 12620-938) at 200 rpm. The matrices were then briefly rinsed in DI water, incubated in m-SBF at 37 °C for 2 days with daily change of m-SBF, and equilibrated in PBS for 6 h.

The mineralized and non-mineralized matrices were sterilized by immersing in 70% ethanol for 6 h. The ethanol-treated matrices were then washed in sterile PBS by replenishing the PBS four times each day for 4 days to fully remove residual ethanol. Sterile non-mineralized and mineralized GelMA-*co*-A6ACA hydrogels were employed for two-dimensional (2-D) culture. Sterile non-mineralized and mineralized GelMA-*co*-A6ACA-*co*-PEGDA macroporous hydrogels were used for three-dimensional (3-D) culture.

2.5. Scanning electron microscopy and energy dispersive spectra

Scanning electron microscopy (SEM) imaging was carried out to investigate the morphology of the mineralized matrices. Energy dispersive spectra (EDS) analysis was performed to determine the composition of the minerals. Samples were briefly rinsed in DI water to remove non-bound ions for 5 min, cut into thin slices and subjected to flash-freezing and lyophilization. After iridium coating for 7 s in the sputter (Emitech, K575X), samples were imaged using SEM (Philips XL30 ESEM) and analyzed for elemental spectra with an integrated EDS system. INCA software was used to quantify Ca/P atomic ratio from elemental spectra. The pore diameter of the macroporous matrices was calculated from either SEM or bright-field images to estimate the pore structures in the dry and wet state, respectively. Roughly 10 pores were chosen from each of three SEM or bright-field images (n = 30) and their diameter was determined using ImageJ. The data are presented as mean ± standard errors.

2.6. Calcium and phosphate assays

Calcium and phosphate assays were conducted to determine the amounts of Ca^{2+} and PO_4^{3-} in the mineralized matrices and to determine the dissolution of the minerals from the mineralized matrices. The matrices were rinsed in DI water, homogenized and freeze-dried, and their dry weights were measured. To measure the Ca^{2+} and PO_4^{3-} contents of the mineralized matrices, the dried matrices were subjected to vigorous shaking in 0.5 M HCl at 25 °C for 3 days. To examine the dissolution of CaP minerals from the mineralized matrices into Ca^{2+} and PO_4^{3-} in an environment lacking these ions, equilibrium swollen matrices were incubated in 1.5 ml of 50 mM Tris buffer (pH = 7.4) at 37 °C for 7 days and 0.3 ml of incubation medium was collected and

replenished with a fresh medium daily. The collected medium was used to measure the dissolution of CaP as a function of the incubation time.

Calcium assay was carried out according to manufacturer's protocol (Calcium reagent set, Pointe Scientific, catalog number: C7503). Briefly, 20 μl of the sample solution was mixed with 1 ml of assay solution containing *o*-cresolphthalein complexone (CPC). The reaction of calcium with CPC gives rise to a purple color. The absorbance of the resultant product was measured at 570 nm using a UV/Vis spectrophotometer (Beckman Coulter, DU 730). The absorbance values were compared with those of standard solution at 0, 5, 10 and 15 mg dl^{-1} of Ca^{2+} in order to determine the Ca^{2+} content of the sample solution.

Phosphate assay was performed as reported elsewhere [37]. Briefly, the assay solution was prepared by mixing 1 part of 10 mM ammonium molybdate, 2 parts of acetone and 1 part of 5 N H_2SO_4 and 125 μl of the sample solution was mixed with 1 ml of assay solution. To this, 100 μl of 1 M citric acid was added. The absorbance of the resulting solution was measured at 380 nm using a UV/Vis spectrophotometer. The PO_4^{3-} concentration in solution was determined using the standard curve for PO_4^{3-}, which was generated for a concentration range of 0–4 mM PO_4^{3-}.

2.7. Degradation

Non-mineralized and mineralized hydrogels (15% GelMA-*co*-9% A6ACA with dimensions 8 mm diameter × 1 mm height) and macroporous hydrogels (10% GelMA-*co*-9%A6ACA-*co*-10% PEGDA with dimensions 5 mm diameter × 2 mm height) were examined for their degradation potential prior to cell cultures. All matrices were dried at 37 °C for 24 h and their dry weights (W_{d0}) were measured. The dried matrices were equilibrated in PBS and incubated in 1.5 ml of 0.02 w/v% collagenase type II (Worthington Biochemical, catalog number: LS004177) in PBS at 37 °C [22]. The matrices incubated in 1.5 ml of PBS under identical experimental conditions were used to examine hydrolytic degradation. The incubation solution was replenished with a fresh solution every other day. After 1, 3, 7 and 14 days of incubation, the matrices were collected and briefly rinsed with PBS for 5 min to remove any soluble components from degraded matrices. The matrices were dried at 37 °C for 24 h, and their weights (W_{dt}) were measured. The weight percentage of the remaining matrix was calculated using the following equation:

$$\text{Weight of remaining matrices } (\%) = \frac{W_{dt}}{W_{d0}} \times 100$$

where W_{d0} and W_{dt} represent the weight of the matrix before and after degradation, respectively.

2.8. Cell culture

The hiPSC line (IMR90p18-iPS) was procured from WiCell Research Institute, which was generated as described elsewhere [38]. The hiPSC were maintained on feeder layers of mitotically inactivated mouse embryonic fibroblasts, using a medium consisting of knockout DMEM (Life Technologies, catalog number: 10829-018), 10 v/v% knockout serum replacement (Life Technologies, catalog number: 10828028), 10 v/v% human plasmanate (Talecris Biotherapeutics), 1 v/v% non-essential amino acids, 1 v/v% penicillin/streptomycin, 1 v/v% Gluta-MAX and 55 μM 2-mercaptoethanol, as previously reported [39]. The medium was changed daily with 30 ng ml^{-1} of bFGF (Life Technologies) supplementation.

Cell culture grade glass coverslips (Fisherbrand, catalog number: 1254582) coated with gelatin (Sigma-Aldrich, catalog number: G9391) was used as a control to compare the cellular behaviors on gelatin-based matrices. The gelatin coating of glass coverslips was carried out by incubating the coverslips with 0.1 w/v% gelatin solution at 37 °C for 3 h. Sterile GelMA-*co*-A6ACA hydrogels and GelMA-*co*-A6ACA-*co*-PEGDA macroporous hydrogels as well as gelatin-coated coverslips were incubated in growth medium composed of DMEM with 10 v/v% FBS (Premium Select; Atlanta Biologicals, catalog number: S11550) at 37 °C for 48 h prior to cell culture.

For 2-D culture, hiPSC were seeded onto non-mineralized and mineralized GelMA-*co*-A6ACA hydrogels and gelatin-coated coverslips at a seeding density of 10,000 cells cm^{-2}. Cells were cultured in 1.5 ml of growth medium (high glucose DMEM containing 5 v/v% FBS and 1 v/v% penicillin/streptomycin) at 37 °C and 5% CO_2. Medium was changed every other day.

For 3-D culture, non-mineralized and mineralized macroporous hydrogels were air-dried at 25 °C for 1 h and 10 μl of cell suspension containing ~300,000 hiPSC was dispensed into the macroporous hydrogels. The hiPSC-seeded matrices were incubated at 37 °C and 5% CO_2 for 2 h for cell infiltration. The matrices infiltrated with the cells were cultured in 1.5 ml of growth medium with media change every other day.

2.9. Cell tracker staining

To visualize cell attachment in 2-D culture, cells were stained with CellTracker (Life Technologies, catalog number: C34552) at 3 days post-plating. Briefly, the cells attached to the matrix were incubated in 20 μM CellTracker reagent in DMEM at 37 °C for 30 min and then in growth medium at 37 °C for an additional 30 min. The stained cells were imaged using a fluorescence microscope (Carl Zeiss, Axio Observer.A1). The images were used to determine the circularity of the cells using the equation below [10]. Ten cells per image from three different images were used to calculate the area (A) and perimeter (p) of the cells to estimate the circularity ($n = 30$).

$$\text{Circularity} = \frac{4\pi A}{p^2}$$

2.10. Reverse transcription-polymerase chain reaction (RT-PCR)

PCR analysis was conducted to evaluate time-dependent changes in gene expressions of hiPSC in 2-D and 3-D cultures. Total RNA was extracted from samples ($n = 3$ per group per time point) using TRIzol according to manufacturer's protocol. For each sample, 1 μg of RNA was used to synthesize cDNA using iScript cDNA synthesis kit (Bio-rad, catalog number: 170-8891) following the manufacturer's protocol. Quantitative RT-PCR measurements were performed using SYBR Select Master Mix (Life Technologies, catalog number: 4472908). In addition to the osteogenic PCR array (SA Biosciences, catalog number: PAHS-026), the gene expression profile for a number of osteogenic markers (RUNX2, OCN and SPP1) and the pluripotency marker (NANOG) as a function of culture time was carried out. The primer sequences are provided in Supplementary Table S1. For the PCR array, 84 gene expressions relevant to osteogenic differentiation were profiled and presented as a heat map. The colors of the heat map were scaled according to the relative expression of hiPSC grown on different matrices (mineralized GelMA-based matrices, non-mineralized GelMA-based matrices, and gelatin-coated coverslips). Red color was assigned to the group with the highest expression, while green color was assigned to the group with the lowest expression. The color between red and green was assigned to the group with the intermediate expression level. For RUNX2, OCN, SPP1 and NANOG, the gene expression was normalized to GAPDH, a housekeeping gene. The expression level of each target gene was calculated as $2^{-\Delta\Delta Ct}$.

The expression level of hiPSC grown on various matrices in 2-D and 3-D cultures was normalized to that of undifferentiated, pluripotent hiPSC and presented as fold expression.

2.11. Immunofluorescent staining

The cells cultured on various matrices were fixed with 4% formaldehyde at 25 °C for 7 min, washed in PBS, and blocked/permeabilized in a blocking solution of PBS containing 3% BSA and 0.1% Triton-X at 25 °C for 30 min. The cells were then incubated with a blocking solution containing primary antibodies against OCT4 (1:200; rabbit polyclonal, Santa Cruz Biotechnology, catalog number: sc-9081), NANOG (1:200; rabbit polyclonal, Santa Cruz Biotechnology, catalog number: sc-33759) or OCN (1:100; mouse monoclonal, Santa Cruz Biotechnology, catalog number: sc-74495) at 4 °C for 16 h. The cells were washed in PBS and incubated in a blocking solution containing secondary antibody raised against rabbit (1:250; Life Technologies, Alexa Flour 647) or mouse (1:250; Life Technologies, Alexa Flour 568) and phalloidin (1:100; Life Technologies, Alexa Flour 488) at 25 °C for 60 min. To counterstain the nuclei, cells were incubated in the Hoechst 33342 solution (2 μg ml^{-1}; Life Technologies) at 25 °C for 7 min. The images were acquired in a linear mode using the same exposure time for all samples. Using ImageJ software, the background of images was identically subtracted from all images by applying a rolling ball algorithm with rolling ball radius of 750 pixels. To examine the autofluorescence of minerals, acellular mineralized matrices were stained at the same time and the images were exposed to the same processing as those with the cells. To evaluate the specificity of osteocalcin antibody, hiPSC cultured on mineralized matrices for 28 days were stained with secondary antibody without the use of primary antibody and the background of images was subtracted using the identical method.

2.12. Live–dead assay

Live–dead assay was carried out to evaluate the viability and distribution of cells within the macroporous hydrogels after 3 days of cell seeding using a Live/Dead Viability/Cytotoxicity kit (Life Technologies, catalog number: L-3224). Briefly, hiPSC-seeded matrices were washed in PBS and cut into thin slabs. These thin slices were stained using a solution composed of DMEM with 0.05 v/v% green-fluorescent calcein-AM and 0.2 v/v% red-fluorescent ethidium homodimer-1 at 37 °C for 30 min. The stained sections were washed with PBS and imaged.

2.13. DNA assay

The hiPSC-seeded macroporous hydrogels were subjected to the DNA assay at 3, 7 and 28 days of culture. The cell-laden matrices were lyophilized and their dry weights were measured. Each lyophilized sample was homogenized in 1 ml of papain solution and incubated at 60 °C for 16 h. The papain solution was prepared by dissolving 125 μg ml^{-1} of papain in a buffer containing 10 mM l-cysteine, 100 mM phosphate and 10 mM ethylenediaminetetraacetic acid (EDTA) at pH 6.3. To measure the DNA contents of the digested sample, a Quant-iT PicoGreen dsDNA assay kit (Life Technologies, catalog number: P11496) was used. One part each of digested samples and PicoGreen dsDNA reagent were mixed. The fluorescence of the resulting solution was measured using a microplate reader (Beckman Coulter, DTX 880). Fluorescence values of the samples were compared with those of Lambda DNA standard to quantify the DNA contents of the experimental samples. The DNA content of each sample was normalized to the corresponding dry weight.

2.14. Immunohistochemical staining

The hiPSC-laden matrices were fixed with 4% paraformaldehyde at 4 °C for 1 day, demineralized in 10% EDTA (pH = 7.3) at 4 °C for 3 h, and equilibrated in PBS for 6 h. Gradual dehydration of the samples was achieved by immersing them in water/ethanol mixtures and then in pure ethanol for 6 h. The dehydrated samples were soaked in Citrisolv solution for 1 h, incubated in a mixture of 95 w/w% paraffin and 5 w/w% poly(ethylene-*co*-vinyl acetate) (PEVA; Sigma Aldrich, catalog number: 437220) liquid at 70 °C under vacuum for 1 day. The specimens were embedded with paraffin–PEVA mixture through solidification at 25 °C for 1 day. The samples were subsequently sectioned into 10 μm-sized slices using a microtome (Leica, RM2255). The sections were placed into DI water at 40 °C for 5 min, then onto charged glass slides, and allowed to dry at 37 °C for 16 h. The sections on the glass slides were immersed in Citrisolv at 60 °C for 15 min with two changes of Citrisolv to remove the paraffin–PEVA mixture. The Citrisolv solution was then replaced with pure ethanol. The samples were progressively hydrated using ethanol/DI water mixtures, followed by DI water.

The sections were incubated in a blocking solution composed of PBS with 3 w/v% BSA and 0.1 v/v% Triton X-100 at 25 °C for 60 min and incubated with primary antibody (diluted in blocking solution) against OCN (1:100, mouse monoclonal, Abcam, catalog number: ab13420) at 4 °C for 16 h. The sections were washed in PBS containing 0.05 v/v% Tween 20 (PBS-Tween 20) three times and treated with 3 v/v% hydrogen peroxide for 7 min to deactivate endogenous peroxidases. The sections were then incubated in a blocking buffer containing horseradish peroxidase-conjugated secondary antibody against mouse (1:100, Santa Cruz Biotechnology, catalog number: sc-2005) at 25 °C for 60 min. The sections were washed in PBS-Tween20 three times and exposed to a developing solution containing 3,3′-diaminobenzidine substrate (Vector Laboratories, catalog number: SK-4100) for 7 min, washed in PBS-Tween 20 three times, and subsequently imaged using a microscope in color mode.

2.15. Statistical analysis

Statistical analyses were performed using GraphPad Prism (version 5.00) software. Statistical significances were assigned for p values <0.05. The asterisks were assigned to further demonstrate different degrees of statistical significance. Three different statistical methods were used to compare groups in various combinations. A two-tailed Student's t-test was employed to compare two groups at the same time point. One-way analysis of variance (ANOVA) with the Tukey–Kramer post-hoc test was used to compare multiple groups at the same time point. Two-way ANOVA with Bonferroni post-hoc test was used to compare multiple groups at various time points.

3. Results

3.1. Synthesis, characterization and degradation of mineralized matrices

Hydrogels and macroporous hydrogels were used for 2-D and 3-D cultures, respectively. The hydrogel and macroporous matrices were mineralized to incorporate calcium phosphate moieties. Both mineralized hydrogels and macroporous hydrogels were found to be opaque, in contrast to the transparent non-mineralized counterparts (Supplementary Figs. S1a, S2a). SEM images of the mineralized hydrogels and macroporous hydrogels showed matrix-bound minerals with a plate-like morphology; no such features were

present in the corresponding non-mineralized controls (Fig. 1a, e). EDS revealed the presence of calcium and phosphorus elements in mineralized matrices with a Ca/P ratio of 0.99 and 1.42 for the mineralized hydrogels and macroporous hydrogels, respectively. As expected, no calcium or phosphorous elements were detected in their non-mineralized counterparts. As evident from Ca^{2+} and PO_4^{3-} measurements, the mineralized hydrogels contained 32.2 ± 1.5 and 50.3 ± 4.8 mg of Ca^{2+} and PO_4^{3-} per gram of dry weight, respectively (Supplementary Fig. S1b, c). Similarly, the mineralized macroporous hydrogels had 68.4 ± 4.2 and 112.3 ± 4.7 mg of Ca^{2+} and PO_4^{3-} per gram of dry weight, respectively (Supplementary Fig. S2c, d). Concurrent with previous findings, the CaP

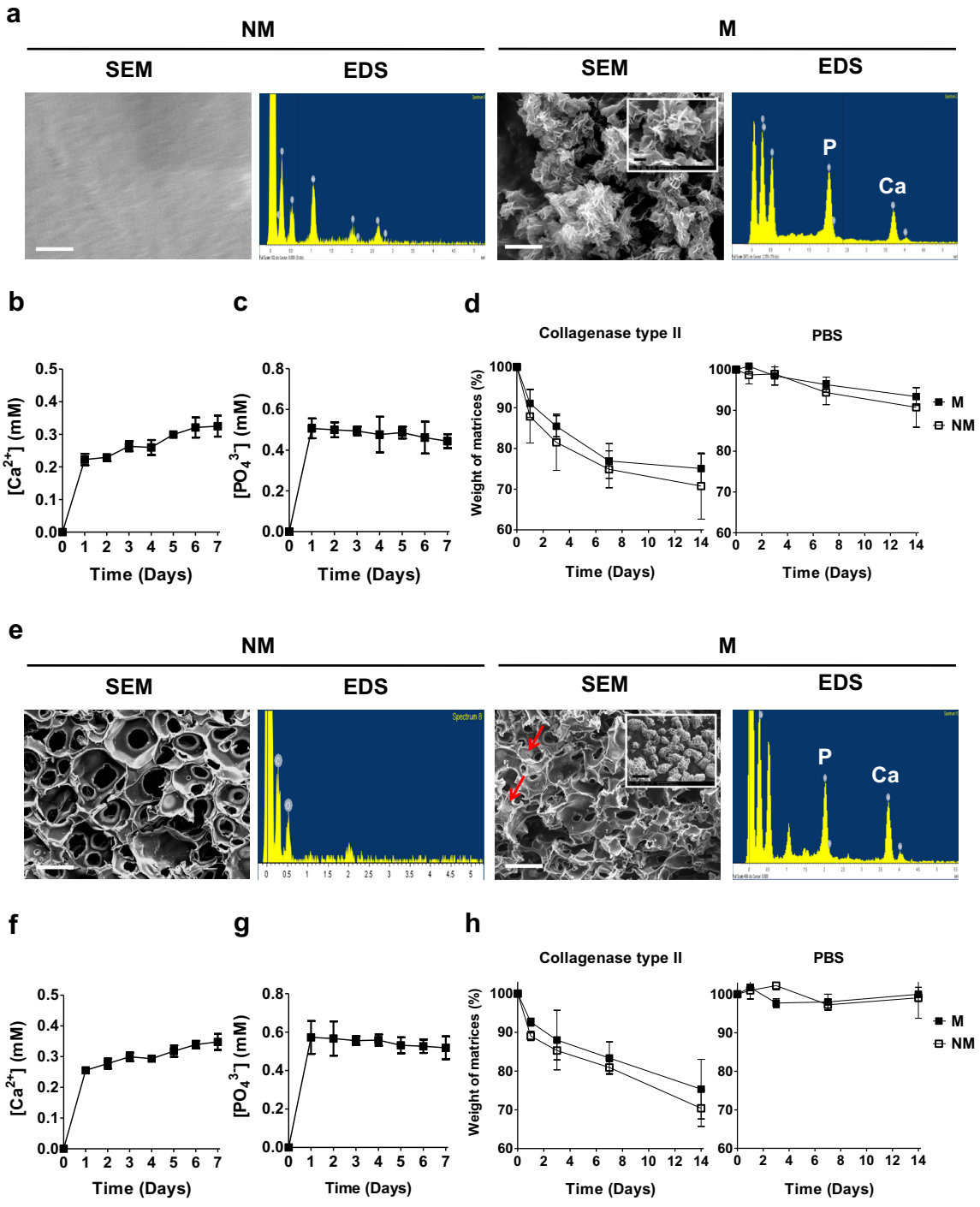

Fig. 1. Development and characterization of GelMA-based matrices. (a) SEM images and corresponding EDS for non-mineralized (NM) and mineralized (M) gelatin-methacrylate-*co*-acryloyl 6-aminocaprioic acid (GelMA-*co*-A6ACA) hydrogels. Scale bar: 1 μm. Inset shows high magnification image. Scale bar: 200 nm. Dissolution of (b) Ca^{2+} and (c) PO_4^{3-} from mineralized GelMA-*co*-A6ACA hydrogels incubated in Tris–HCl buffer at 37 °C as a function of time. (d) *In vitro* degradation of non-mineralized and mineralized GelMA-*co*-A6ACA hydrogels in 0.02 w/v% collagenase type II solution or PBS at 37 °C as a function of time. (e) SEM images and corresponding EDS for non-mineralized and mineralized GelMA-*co*-A6ACA-*co*-PEGDA macroporous hydrogels. Red arrows indicate mineral structures. Scale bar: 100 μm. Inset shows high magnification image. Scale bar: 1 μm. Release of (f) Ca^{2+} and (g) PO_4^{3-} from mineralized GelMA-*co*-A6ACA-*co*-PEGDA macroporous hydrogels in Tris–HCl buffer at 37 °C as a function of time. (h) *In vitro* degradation of non-mineralized and mineralized GelMA-*co*-A6ACA-*co*-PEGDA macroporous hydrogels in 0.02 w/v% collagenase type II solution or PBS at 37 °C as a function of time. Data are presented as mean ± standard errors (n = 3).

moieties of the mineralized matrices (mineralized hydrogels and macroporous hydrogels) dissociated into Ca^{2+} and PO_4^{3-} ions in a medium lacking these components (Fig. 1b, c, f, g) [17]. Both mineralized hydrogels and macroporous hydrogels exhibited a rapid release of Ca^{2+} and PO_4^{3-} ions within 1 day, followed by slow release of Ca^{2+} and no significant release of PO_4^{3-} for 7 days.

Both non-mineralized and mineralized macroporous hydrogels exhibited interconnected pores, as evident from the SEM images (Fig. 1e). Furthermore, the pore diameter of the macroporous hydrogels in their dried state, estimated from the SEM images, was 50.2 ± 3.0 μm. The pore diameter of the non-mineralized and mineralized macroporous hydrogels in their swollen state, estimated from the bright-field images, was 117.7 ± 5.7 and 115.2 ± 6.4 μm, respectively (Supplementary Fig. S2b).

The ability to degrade in the presence of collagenase is a characteristic of gelatin-based scaffolds. To evaluate the effect of mineralization on the degradation of GelMA-based matrices, the mineralized and non-mineralized hydrogels and macroporous hydrogels were incubated in PBS or PBS containing collagenase type II. Enzymatic degradation of non-mineralized and mineralized GelMA-based hydrogels with collagenase type II resulted in ~29% and 25% of mass loss by 14 days, respectively, while their incubation in PBS exhibited <10% of mass loss during the same time period (Fig. 1d). A similar degradation pattern was observed for macroporous hydrogels (Fig. 1h). Enzyme-mediated degradation of non-mineralized and mineralized GelMA-based macroporous hydrogels yielded ~30% and 25% of mass loss after 14 days of incubation in collagenase type II, respectively. The hydrolytic degradation of such macroporous matrices was found to be negligible during 14 days of incubation in PBS.

3.2. Attachment, proliferation and osteogenic differentiation of hiPSC on mineralized matrices in 2-D culture

The pluripotency of hiPSC prior to their culture on various matrices was confirmed by immunofluorescent staining for OCT4 and NANOG, well-established pluripotent markers (Supplementary Fig. S3) [39]. The pluripotent hiPSC were seeded onto mineralized and non-mineralized GelMA-*co*-A6ACA hydrogel matrices as well as gelatin-coated coverslips. The adhesion and growth of hiPSC on mineralized GelMA-*co*-A6ACA hydrogels were examined and compared against those on non-mineralized hydrogels and gelatin-coated coverslips as a function of culture time (Fig. 2a, b). All matrices supported the attachment of hiPSC within 3 days of culture with no significant differences in cell adhesion (Fig. 2a). The cell shape measured in terms of circularity suggests that cells on all matrices spread and acquired a similar shape within 3 days of plating (Fig. 2b). By 10 days of culture, hiPSC on all the matrices grew to reach confluence (Fig. 2a). Following verification that all matrices under investigation support the attachment and proliferation of hiPSC in similar extents, the osteogenic differentiation of hiPSC on various matrices was evaluated. After 28 days of culture, a PCR array revealed that the cells on mineralized matrices exhibited an up-regulation of various genes relevant to cells undergoing osteogenesis compared with those on non-mineralized matrices and gelatin-coated coverslips (Fig. 3a). The gene profile was further verified through time course analyses of different osteogenic gene markers and it was found that the cells on mineralized matrices showed higher expression of RUNX2, OCN and SPP1 compared with those on non-mineralized and coverslip groups throughout 28 days of culture (Fig. 3b–d). Immunofluorescent staining for OCN in hiPSC on mineralized hydrogels revealed positive staining after 28 days of culture, which was not detected on non-mineralized hydrogels or coverslips (Fig. 3e and Supplementary Fig. S4). Moreover, OCN staining intensity was found to gradually increase for hiPSC on mineralized hydrogels with culture time (Supplementary Fig. S5a). The

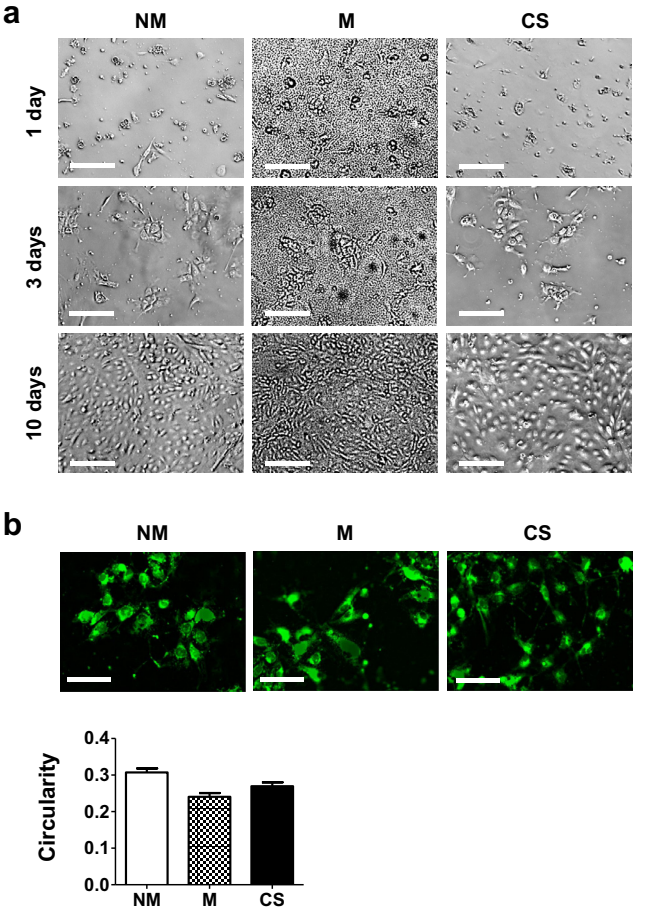

Fig. 2. Attachment and proliferation of hiPSC on different matrices. (a) Bright-field images for hiPSC after 1, 3 and 10 days of culture on non-mineralized (NM) and mineralized (M) hydrogels and gelatin-coated coverslips (CS). Scale bar: 200 μm. (b) Images of hiPSC labeled using CellTracker after 3 days of culture on non-mineralized and mineralized hydrogels and coverslips. Scale bar: 100 μm. The bar graph shows the quantitative representation of the circularity; the circularity indices were determined from the stained images. Data are shown as mean ± standard errors (n = 30).

corresponding Hoechst and F-actin staining of the cells on various matrices as a function of culture time are also shown (Supplementary Fig. S5a, b). The hiPSC cultured on all matrices exhibited the down-regulation of NANOG expression compared with pluripotent hiPSC prior to their culture on various matrices (Supplementary Fig. S5c).

3.3. Osteogenic differentiation of hiPSC on mineralized macroporous matrices in 3-D culture

The potential of 3-D mineralized matrices in directing osteogenic commitment of hiPSC was next determined using mineralized GelMA-*co*-A6ACA-*co*-PEGDA macroporous hydrogels. The PEGDA molecules were incorporated to optimize pore interconnectivity and robustness of the macroporous matrices. The mineralized matrix-induced osteogenic differentiation was compared against that of corresponding non-mineralized macroporous hydrogels. Live–dead staining of hiPSC-laden matrices after 3 days of cell seeding demonstrated homogeneous distribution for a majority of live cells within the non-mineralized and mineralized matrices (Fig. 4a). While both matrices supported cell survival, there were distinct differences in cell shape and cell–matrix interactions. Most cells within the non-mineralized matrices were

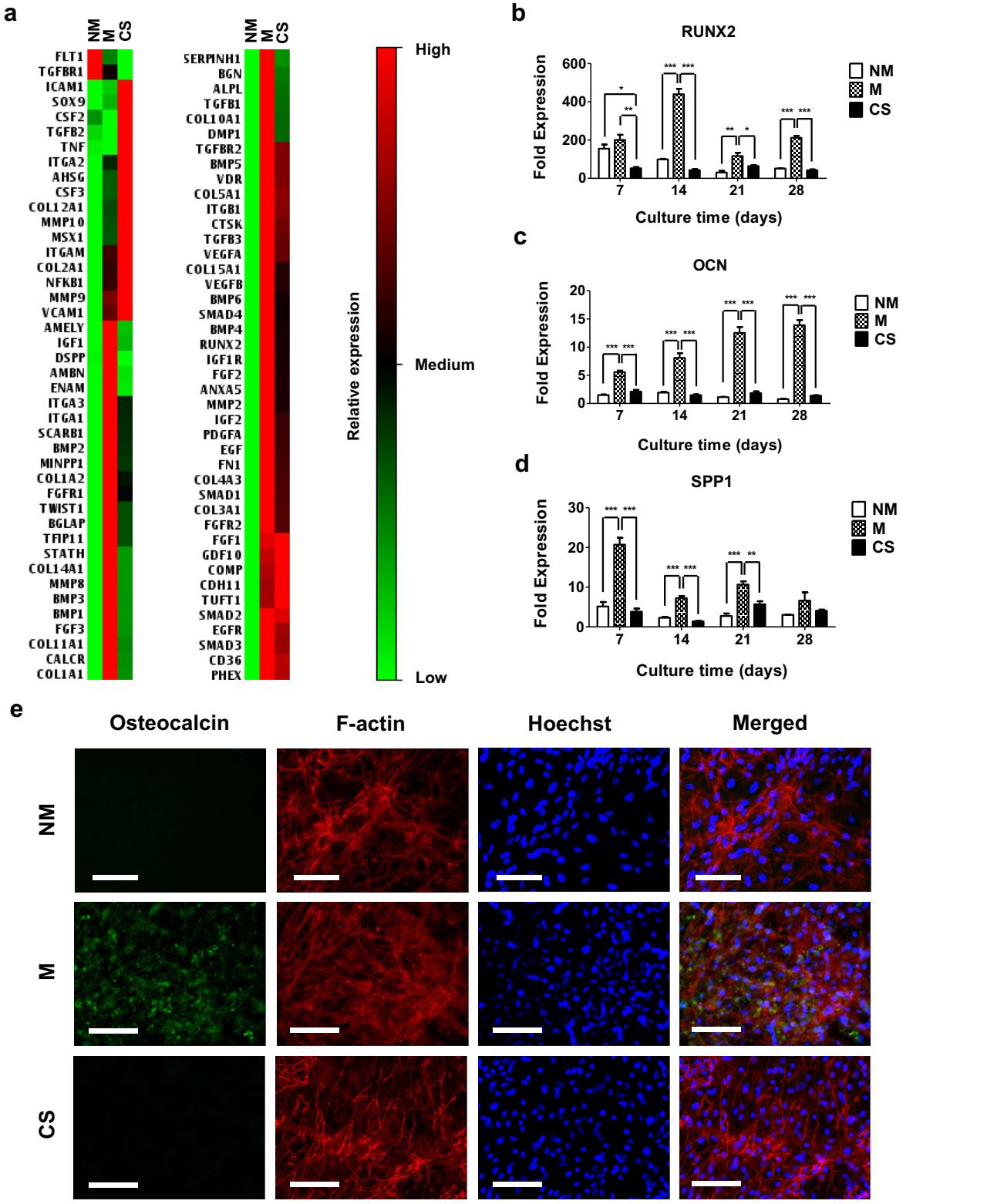

Fig. 3. Osteogenic differentiation of hiPSC on CaP-rich mineralized hydrogels in 2-D culture. (a) Gene expression array analyses of hiPSC cultured for 28 days on non-mineralized (NM) and mineralized (M) hydrogels and coverslips (CS). Relative expressions: red (high), black (medium) and green (low). Gene expressions of (b) RUNX2, (c) OCN and (d) SPP1 for hiPSC cultured on non-mineralized and mineralized hydrogels and coverslips as a function of culture time. Data are presented as fold expression of target genes after normalization to undifferentiated, pluripotent hiPSC. (e) Immunofluorescent staining for OCN (green) and F-actin (red) of hiPSC cultured on non-mineralized and mineralized hydrogels and coverslips for 28 days. Nuclei are stained blue with Hoechst. Scale bars represent 100 μm. Data are displayed as mean ± standard errors (n = 3). (b–d) Comparison of multiple groups at the same time point was made by one-way ANOVA with the Tukey–Kramer post-hoc test. Asterisks indicate statistical significances corresponding to p values ($^{*}p < 0.05$; $^{**}p < 0.01$; $^{***}p < 0.001$).

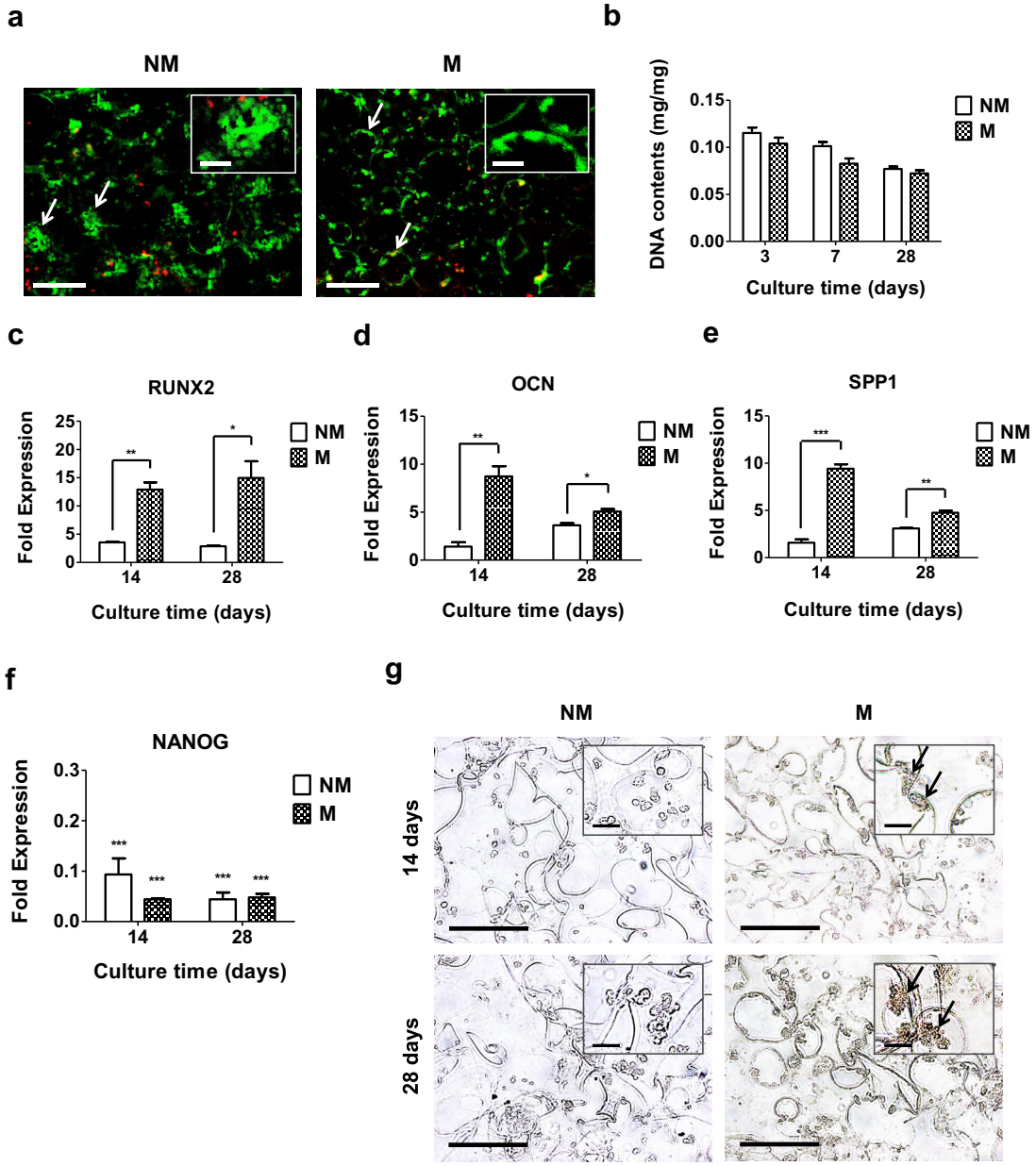

Fig. 4. Osteogenic differentiation of hiPSC on CaP-rich mineralized macroporous hydrogels in 3-D culture. (a) Live-dead staining of hiPSC-laden non-mineralized (NM) and mineralized (M) macroporous hydrogels after 3 days of culture. Arrows and inset indicate aggregated and spread hiPSC within the non-mineralized and mineralized matrices, respectively. Scale bars represent 200 μm, and scale bars in the inset indicate 50 μm. (b) DNA contents of hiPSC cultured using non-mineralized and mineralized matrices as a function of culture time. Data are presented as DNA contents after normalization to dry weight of matrices. Gene expression of (c) RUNX2, (d) OCN, (e) SPP1 and (f) NANOG of hiPSC on non-mineralized and mineralized matrices as a function of culture time. Data are presented as fold expression of target genes after normalization to undifferentiated, pluripotent hiPSC. (g) Immunohistochemical staining for OCN of hiPSC on non-mineralized and mineralized matrices as a function of culture time. Scale bars represent 100 μm. Inset shows high magnification images. Arrows indicate positive stains. Scale bars in the inset represent 20 μm. Data are displayed as mean ± standard errors ($n = 3$). (c–e) Two groups at the same time point were compared by two-tailed Student's t-test. (f) All the groups were compared with undifferentiated, pluripotent hiPSC prior to their culture on all matrices by two-way ANOVA with the Bonferroni post-hoc test. Asterisks represent statistical significances according to p-values. ($^{*}p < 0.05$; $^{**}p < 0.01$; $^{***}p < 0.001$).

aggregated to form small clusters, while those within the mineralized matrices were found to spread on the pore walls of the matrices. Despite the differences in cell shape and adhesion between two matrices, DNA assay showed similar DNA contents of hiPSC cultured in both non-mineralized and mineralized matrices at all experimental time points, suggesting that similar cell numbers were maintained between the mineralized and non-mineralized matrices (Fig. 4b). Time-resolved gene expression of osteogenic markers for RUNX2, OCN and SPP1 revealed significant up-regulation of these markers in cells on mineralized matrices compared with those on non-mineralized matrices, akin to 2-D culture (Fig. 4c–e). Immunohistochemical staining for OCN further corroborated the gene expression pattern, as prevalent staining for OCN was observed in mineralized matrices, which remained absent in non-mineralized counterparts (Fig. 4g). Furthermore, pervasiveness of OCN stains in mineralized matrices progressively increased with culture time. Although only the hiPSC on mineralized macroporous matrices were found to differentiate into osteoblasts, cells cultured in all macroporous matrices showed a significant down-regulation of NANOG expression, similar to 2-D culture (Fig. 4f).

4. Discussion

The potential of biomaterials in directing stem cell differentiation continues to be revealed, leading to new possibilities in regenerative medicine. Human pluripotent stem cells, such as hiPSC, which offer a unique cell source, in conjunction with biomaterials, could be powerful in treating compromised tissue and organs. Studies over the years have designed biomaterials with defined physicochemical cues to direct differentiation of stem cells into targeted phenotypes. Previously, it was shown that biomaterials containing CaP moieties promote osteogenic commitment of stem cells both *in vitro* and *in vivo* [10,11,17]. Here, by employing a mineralized GelMA-based matrix, the present authors ask whether matrix-based cues alone can direct differentiation of pluripotent hiPSC into osteoblasts.

hiPSC grown on GelMA-based matrices in 2-D culture demonstrated similar levels of attachment, spreading and proliferation in growth medium. Though all the matrices supported the adhesion and growth of hiPSC to similar extents, only the cells on mineralized matrices were found to undergo osteogenic differentiation. hiPSC on mineralized matrices after 28 days of culture in a 2-D setting demonstrated intense staining for OCN, an osteoblast marker, coincident with F-actin staining in a majority of the cells. This finding suggests efficient osteogenic differentiation of hiPSC in a mineralized environment. Previous studies demonstrated that biomaterial-assisted osteogenic differentiation of stem cells in 2-D culture was accompanied by changes in cell shape [40]. However, the present findings that cells only on the mineralized matrices underwent osteogenic differentiation, despite cells on all matrices having a similar shape, suggest that the observed osteogenic differentiation of hiPSC on mineralized matrices is not attributed to the cell shape. This finding further implies that the osteogenic differentiation of hiPSC observed on mineralized matrices is attributed mainly to the mineral environment-mediated differentiation cues. Similar results were also observed with 3-D culture, albeit within disparate spatial geometry in the culture. The findings that hiPSC undergo osteogenic differentiation on CaP-rich GelMA-based matrices in 2-D and 3-D culture conditions are consistent with previous findings that CaP-rich PEGDA-based matrices promote osteogenic differentiation of hMSC and hESC [10,11,17]. Together, these studies suggest that mineralized matrices containing CaP moieties offer a robust environment to support osteogenic commitment of stem cells, despite the differences in the organic moieties of the scaffold.

In contrast to 2-D culture, cells in 3-D macroporous hydrogels showed significant differences in their attachment; cells on mineralized matrices exhibited more spread morphology, whereas those on non-mineralized matrices showed aggregation. These results suggest enhanced cell–matrix interactions on mineralized macroporous matrices compared with their non-mineralized counterparts. The reason behind the observed difference between 2-D and 3-D cultures is not apparent. The hiPSC cultured in all matrices showed significant down-regulation of NANOG expression, indicating that all the matrices and culture conditions used in this study are not conducive for the maintenance of pluripotency. This is in agreement with previous studies that showed the importance of a delicate balance in physicochemical cues of the matrix on the maintenance of pluripotency for hiPSC [39].

Although a number of studies have shown that materials containing CaP moieties promote osteogenic differentiation of progenitor cells and contribute to *in vivo* bone tissue repair, recent studies suggest that the osteoinductive function of such matrices is dependent upon their ability to regulate extracellular Ca^{2+} and PO_4^{3-} [9,12]. This could partially explain the different extents of osteogenic outcomes observed among CaP-based matrices with different levels of crystallinity and composition, owing to disparate dissociation kinetics of CaP minerals into Ca^{2+} and PO_4^{3-}. Osathanon et al. [41] previously reported that CaP-rich biomineralized matrices exhibiting faster dissolution rates have a higher osteostimulatory effect on osteoblast-like cells compared with hydroxyapatite-incorporated matrices. Results from the present authors' dissolution studies suggest that the CaP minerals of the mineralized matrices readily dissociate into Ca^{2+} and PO_4^{3-} ions in a permissive environment. The extracellular Ca^{2+} and PO_4^{3-} ions have been shown to promote osteogenic commitment of stem cells through various signaling pathways. Studies by Wen et al. [42] have shown that extracellular Ca^{2+} promotes osteogenic differentiation of MSC through L-type calcium channels. Recently, the present authors have shown that mineralized matrices containing CaP moieties could direct osteogenic differentiation of stem cells through adenosine signaling [43]. In addition, the dissolution and re-precipitation of CaP minerals can adsorb and release osteoinductive growth factors [44–46]. All these factors could be contributing to the observed CaP-bearing matrices-induced osteogenic commitment of hiPSC.

5. Conclusion

In summary, the results described in this study show that mineralized GelMA-based matrices containing CaP mineral direct osteogenic differentiation commitment of hiPSC in growth medium lacking osteoinductive soluble factors. To the present authors' knowledge, this is the first demonstration of osteogenic differentiation of hiPSC by inherent material-based cues. Future work includes the transplantation of hiPSC with GelMA-based matrices *in vivo* to study the effect of minerals and degradation on the osteogenic differentiation of hiPSC and bone tissue formation.

Conflict of interest

Authors declare no conflict of interest.

Acknowledgements

The authors gratefully acknowledge the financial support from National Institutes of Health and California Institute of Regenerative Medicine (NIH, Grant 1 R01 AR063184-01A1; CIRM, RN2-00945 and RT2-01889).

Appendix A. Figures with essential color discrimination

Certain figures in this article, particularly Figs. 1–4 are difficult to interpret in black and white. The full color images can be found in the on-line version, at http://dx.doi.org/10.1016/j.actbio.2014.08.010.

Appendix B. Supplementary data

Supplementary data associated with this article can be found, in the online version, at http://dx.doi.org/10.1016/j.actbio.2014.08.010.

References

[1] Amabile G, Meissner A. Induced pluripotent stem cells: current progress and potential for regenerative medicine. Trends Mol Med 2009;15:59–68.
[2] Wobus AM, Boheler KR. Embryonic stem cells: prospects for developmental biology and cell therapy. Physiol Rev 2005;85:635–78.
[3] Takahashi K, Tanabe K, Ohnuki M, Narita M, Ichisaka T, Tomoda K, et al. Induction of pluripotent stem cells from adult human fibroblasts by defined factors. Cell 2007;131:861–72.

[4] Teng S, Liu C, Krettek C, Jagodzinski M. The application of induced pluripotent stem cells for bone regeneration: current progress and prospects. Tissue Eng Part B Rev 2014;20:328–39.
[5] Illich DJ, Demir N, Stojković M, Scheer M, Rothamel D, Neugebauer J, et al. Concise review: induced pluripotent stem cells and lineage reprogramming: prospects for bone regeneration. Stem Cells 2011;29:555–63.
[6] Discher DE, Mooney DJ, Zandstra PW. Growth factors, matrices, and forces combine and control stem cells. Science 2009;324:1673–7.
[7] Hwang Y, Phadke A, Varghese S. Engineered microenvironments for self-renewal and musculoskeletal differentiation of stem cells. Regen Med 2011;6:505–24.
[8] Saha K, Pollock JF, Schaffer DV, Healy KE. Designing synthetic materials to control stem cell phenotype. Curr Opin Chem Biol 2007;11:381–7.
[9] LeGeros RZ. Calcium phosphate-based osteoinductive materials. Chem Rev 2008;108:4742–53.
[10] Phadke A, Shih YR, Varghese S. Mineralized synthetic matrices as an instructive microenvironment for osteogenic differentiation of human mesenchymal stem cells. Macromol Biosci 2012;12:1022–32.
[11] Phadke A, Hwang Y, Hee Kim S, Hyun Kim S, Yamaguchi T, Masuda K, et al. Effect of scaffold microarchitecture on osteogenic differentiation of human mesenchymal stem cells. Eur Cell Mater 2013;25:114–29.
[12] Yuan H, Fernandes H, Habibovic P, de Boer J, Barradas AM, de Ruiter A, et al. Osteoinductive ceramics as a synthetic alternative to autologous bone grafting. Proc Natl Acad Sci USA 2010;107:13614–9.
[13] Vaquette C, Ivanovski S, Hamlet SM, Hutmacher DW. Effect of culture conditions and calcium phosphate coating on ectopic bone formation. Biomaterials 2013;34:5538–51.
[14] Seyedjafari E, Soleimani M, Ghaemi N, Shabani I. Nanohydroxyapatite-coated electrospun poly (l-lactide) nanofibers enhance osteogenic differentiation of stem cells and induce ectopic bone formation. Biomacromolecules 2010;11:3118–25.
[15] Song G, Habibovic P, Bao C, Hu J, van Blitterswijk CA, Yuan H, et al. The homing of bone marrow MSCs to non-osseous sites for ectopic bone formation induced by osteoinductive calcium phosphate. Biomaterials 2013;34:2167–76.
[16] Phadke A, Zhang C, Hwang Y, Vecchio K, Varghese S. Templated mineralization of synthetic hydrogels for bone-like composite materials: role of matrix hydrophobicity. Biomacromolecules 2010;11:2060–8.
[17] Kang H, Wen C, Hwang Y, Shih Y-RV, Kar M, Seo SW, et al. Biomineralized matrix-assisted osteogenic differentiation of human embryonic stem cells. J Mater Chem B 2014;2:5676–88.
[18] Heino J. The collagen family members as cell adhesion proteins. BioEssays 2007;29:1001–10.
[19] Hutson CB, Nichol JW, Aubin H, Bae H, Yamanlar S, Al-Haque S, et al. Synthesis and characterization of tunable poly (ethylene glycol): gelatin methacrylate composite hydrogels. Tissue Eng Part A 2011;17:1713–23.
[20] Chen YC, Lin RZ, Qi H, Yang Y, Bae H, Melero-Martin JM, et al. Functional human vascular network generated in photocrosslinkable gelatin methacrylate hydrogels. Adv Funct Mater 2012;22:2027–39.
[21] Talwar R, Di Silvio L, Hughes FJ, King GN. Effects of carrier release kinetics on bone morphogenetic protein-2-induced periodontal regeneration in vivo. J Clin Periodontol 2001;28:340–7.
[22] Park KM, Lee Y, Son JY, Oh DH, Lee JS, Park KD. Synthesis and characterizations of in situ cross-linkable gelatin and 4-arm-PPO–PEO hybrid hydrogels via enzymatic reaction for tissue regenerative medicine. Biomacromolecules 2012;13:604–11.
[23] Benton JA, DeForest CA, Vivekanandan V, Anseth KS. Photocrosslinking of gelatin macromers to synthesize porous hydrogels that promote valvular interstitial cell function. Tissue Eng Part A 2009;15:3221–30.
[24] Yaylaoğlu M, Korkusuz P, Örs Ü, Korkusuz F, Hasirci V. Development of a calcium phosphate–gelatin composite as a bone substitute and its use in drug release. Biomaterials 1999;20:711–9.
[25] Nichol JW, Koshy ST, Bae H, Hwang CM, Yamanlar S, Khademhosseini A. Cell-laden microengineered gelatin methacrylate hydrogels. Biomaterials 2010;31:5536–44.
[26] Zou L, Luo Y, Chen M, Wang G, Ding M, Petersen CC, et al. A simple method for deriving functional MSCs and applied for osteogenesis in 3D scaffolds. Sci Rep 2013;3.
[27] de Peppo GM, Marcos-Campos I, Kahler DJ, Alsalman D, Shang L, Vunjak-Novakovic G, et al. Engineering bone tissue substitutes from human induced pluripotent stem cells. Proc Natl Acad Sci USA 2013;110:8680–5.
[28] Ardeshirylajimi A, Dinarvand P, Seyedjafari E, Langroudi L, Adegani FJ, Soleimani M. Enhanced reconstruction of rat calvarial defects achieved by plasma-treated electrospun scaffolds and induced pluripotent stem cells. Cell Tissue Res 2013;354:849–60.
[29] Ardeshirylajimi A, Hosseinkhani S, Parivar K, Yaghmaie P, Soleimani M. Nanofiber-based polyethersulfone scaffold and efficient differentiation of human induced pluripotent stem cells into osteoblastic lineage. Mol Biol Rep 2013;40:4287–94.
[30] Kang R, Luo Y, Zou L, Xie L, Lysdahl H, Jiang X, et al. Osteogenesis of human induced pluripotent stem cells derived mesenchymal stem cells on hydroxyapatite contained nanofibers. RSC Adv 2014;4:5734–9.
[31] Liu J, Chen W, Zhao Z, Xu HH. Reprogramming of mesenchymal stem cells derived from iPSCs seeded on biofunctionalized calcium phosphate scaffold for bone engineering. Biomaterials 2013;34:7862–72.
[32] Levi B, Hyun JS, Montoro DT, Lo DD, Chan CK, Hu S, et al. In vivo directed differentiation of pluripotent stem cells for skeletal regeneration. Proc Natl Acad Sci USA 2012;109:20379–84.
[33] Hwang Y, Zhang C, Varghese S. Poly (ethylene glycol) cryogels as potential cell scaffolds: effect of polymerization conditions on cryogel microstructure and properties. J Mater Chem 2010;20:345–51.
[34] Ayala R, Zhang C, Yang D, Hwang Y, Aung A, Shroff SS, et al. Engineering the cell–material interface for controlling stem cell adhesion, migration, and differentiation. Biomaterials 2011;32:3700–11.
[35] Bryant SJ, Cuy JL, Hauch KD, Ratner BD. Photo-patterning of porous hydrogels for tissue engineering. Biomaterials 2007;28:2978–86.
[36] Oyane A, Kim HM, Furuya T, Kokubo T, Miyazaki T, Nakamura T. Preparation and assessment of revised simulated body fluids. J Biomed Mater Res, Part A 2003;65:188–95.
[37] Heinonen JK, Lahti RJ. A new and convenient colorimetric determination of inorganic ortho-phosphate and its application to the assay of inorganic pyrophosphatase. Anal Biochem 1981;113:313–7.
[38] Yu J, Vodyanik MA, Smuga-Otto K, Antosiewicz-Bourget J, Frane JL, Tian S, et al. Induced pluripotent stem cell lines derived from human somatic cells. Science 2007;318:1917–20.
[39] Chang CW, Hwang Y, Brafman D, Hagan T, Phung C, Varghese S. Engineering cell–material interfaces for long-term expansion of human pluripotent stem cells. Biomaterials 2013;34:912–21.
[40] McBeath R, Pirone DM, Nelson CM, Bhadriraju K, Chen CS. Cell shape, cytoskeletal tension, and RhoA regulate stem cell lineage commitment. Dev Cell 2004;6:483–95.
[41] Osathanon T, Linnes ML, Rajachar RM, Ratner BD, Somerman MJ, Giachelli CM. Microporous nanofibrous fibrin-based scaffolds for bone tissue engineering. Biomaterials 2008;29:4091–9.
[42] Wen L, Wang Y, Wang H, Kong L, Zhang L, Chen X, et al. L-type calcium channels play a crucial role in the proliferation and osteogenic differentiation of bone marrow mesenchymal stem cells. Biochem Biophys Res Commun 2012;424:439–45.
[43] Shih Y-RV, Hwang Y, Phadke A, Kang H, Hwang NS, Caro EJ, et al. Calcium phosphate-bearing matrices induce osteogenic differentiation of stem cells through adenosine signaling. Proc Natl Acad Sci USA 2014;111:990–5.
[44] Suarez-Gonzalez D, Barnhart K, Migneco F, Flanagan C, Hollister SJ, Murphy WL. Controllable mineral coatings on PCL scaffolds as carriers for growth factor release. Biomaterials 2012;33:713–21.
[45] Suárez-González D, Lee JS, Lan Levengood SK, Vanderby Jr R, Murphy WL. Mineral coatings modulate β-TCP stability and enable growth factor binding and release. Acta Biomater 2012;8:1117–24.
[46] Autefage H, Briand-Mesange F, Cazalbou S, Drouet C, Fourmy D, Goncalves S, et al. Adsorption and release of BMP-2 on nanocrystalline apatite-coated and uncoated hydroxyapatite/beta-tricalcium phosphate porous ceramics. J Biomed Mater Res B Appl Biomater 2009;91:706–15.